

NOTICE: This is the author's version of a work that was accepted by *Journal of Systems and Software* in July 2007. Changes resulting from the publishing process, such as peer review, editing, corrections, structural formatting, and other quality control mechanisms may not be reflected in this document. Changes may have been made to this work since it was submitted for publication. A definitive version has been published in *Journal of Systems and Software*, vol. 81, no. 7, pp. 1130-1143, 2008, DOI: 10.1016/j.jss.2007.07.037.

Cryptanalysis of the RCES/RSES Image Encryption Scheme

Shujun Li ^{a,*}, Chengqing Li ^b, Guanrong Chen ^b and Kwok-Tung Lo ^c

^a*FernUniversität in Hagen, Lehrgebiet Informationstechnik, Universitätsstraße 27, 58084 Hagen, Germany*

^b*Department of Electronic Engineering, City University of Hong Kong, 83 Tat Chee Avenue, Kowloon Tong, Hong Kong SAR, China*

^c*Department of Electronic and Information Engineering, The Hong Kong Polytechnic University, Hung Hom, Kowloon, Hong Kong SAR, China*

Abstract

Recently, a chaos-based image encryption scheme called RCES (also called RSES) was proposed. This paper analyzes the security of RCES, and points out that it is insecure against the known/chosen-plaintext attacks: the number of required known/chosen plain-images is only one or two. In addition, the security of RCES against the brute-force attack was overestimated. Both theoretical and experimental analyses are given to show the performance of the suggested known/chosen-plaintext attacks. The insecurity of RCES is due to its special design, which makes it a typical example of insecure image encryption schemes. Some lessons are drawn from RCES to show some common principles for ensuring the high level of security of an image encryption scheme.

Key words: image encryption, chaotic cryptography, RCES/RSES, cryptanalysis, known-plaintext attack, chosen-plaintext attack, CKBA

* Corresponding author: Shujun Li (<http://www.hooklee.com>).

1 Introduction

In the digital world today, the security of digital images becomes more and more important, since the communications of digital products over networks occur more and more frequently. Furthermore, special and reliable security in storage and transmission of digital images is needed in many applications, such as pay-TV, medical imaging systems, military image database and communications as well as confidential video conferencing, etc. In recent years, some consumer electronic devices, especially mobile phones and hand-held devices, have also started to provide the function of saving and exchanging digital images via the support of multimedia messaging services over wireless networks.

To meet the challenges arising from different applications, good encryption of digital images is necessary. The simplest way to encrypt an image is to consider the 2-D image stream as a 1-D data stream, and then encrypt this 1-D stream with any available cipher [1]. Although such a simple way is sufficient to protect digital images in some civil applications, encryption schemes considering special features of digital images, such as the bulky size and the large redundancy in uncompressed images, are still needed to provide better overall performance and make the adoption of the encryption scheme easier in the whole image processing system.

Since the 1990s, many specific algorithms have been proposed, aiming to provide better solutions to image encryption [2–22]. At the same time, cryptanalytic work on proposed image encryption schemes has also been developed, and some existing schemes have been found to be insecure from the cryptographic point of view [23–32]. Due to the tight relationship between chaos and cryptography [33, Chap. 2], chaotic systems have been widely used in image encryption to realize diffusion and confusion in a good cipher [9–12, 16–20]. For a more comprehensive survey of the state of the art about image encryption schemes, see [34–36].

The present paper focuses on a new chaos-based image encryption scheme proposed by Chen and Yen in [19, 20], which was originally called RSES (random seed encryption system) in [19] and then renamed to be RCES (random control encryption system) in [20]. RCES can be considered as an enhanced version of a previously-proposed image encryption scheme called CKBA (chaotic key-based algorithm) [18], which has been cryptanalyzed in [28]. The present paper evaluates the security of RCES, and points out that RCES is as weak as CKBA, though it seems more complicated than CKBA. In known/chosen-plaintext attack, only one or two known/chosen plain-images are enough to break this image encryption scheme. In addition, we also show that the security of RCES against brute-force attack was much overestimated by Chen and

Yen in [19, 20].

Due to the special design of RCES, some of its essential security defects are very useful for revealing several general principles of designing secure image encryption schemes. This magnifies the cryptanalysis presented below, though RCES is not a very delicate cipher from the cryptographical point of view.

This paper is organized as follows. Section 2 briefly introduces RCES and its parent version CKBA. A detailed cryptanalysis of RCES is presented in Sec. 3, where some experimental results are given to support the theoretical analysis. Section 4 discusses some design principles drawn from the essential security defects of RCES. The last section concludes the paper.

2 Introduction to RCES

2.1 CKBA [18] - The Parent Version of RCES

Assume that the size of the plain-image for encryption is $M \times N^1$, CKBA can be described as follows.

2.1.1 The secret key

The secret key includes two bytes $key1$, $key2$, and the initial condition $x(0) \in (0, 1)$ of the following chaotic Logistic map:

$$x(n+1) = \mu \cdot x(n) \cdot (1 - x(n)), \quad (1)$$

which is a well-studied chaotic system in chaos theory and behaves chaotically when $\mu > 3.5699 \dots$ [37].

2.1.2 Initialization

Run the chaotic system to generate a chaotic sequence, $\{x(i)\}_{i=0}^{\lceil MN/8 \rceil - 1}$, where $\lceil a \rceil$ denotes the smallest integer that is not less than a . From the 16-bit binary representation of $x(i) = 0.b(16i+0)b(16i+1) \dots b(16i+15)$, derive a pseudo-random binary sequence (PRBS), $\{b(i)\}_{i=0}^{2MN-1}$.

¹ In this paper, $M \times N$ is in the form “width×height”.

2.1.3 Encryption

For the plain-pixel $f(x, y)$ ($0 \leq x \leq M - 1, 0 \leq y \leq N - 1$), the corresponding cipher-pixel $f'(x, y) = f'(x, y)$ is determined by the following rule:

$$f'(x, y) = \begin{cases} f(x, y) \oplus key1, & B(x, y) = 3, \\ f(x, y) \odot key1, & B(x, y) = 2, \\ f(x, y) \oplus key2, & B(x, y) = 1, \\ f(x, y) \odot key2, & B(x, y) = 0, \end{cases} \quad (2)$$

where $B(x, y) = 2 \times b(x \times N + y) + b(x \times N + y + 1)$, and \oplus and \odot denote XOR and XNOR operations, respectively. Since $a \odot b = \overline{a \oplus b} = a \oplus \bar{b}$, the above equation is equivalent to

$$f'(x, y) = \begin{cases} f(x, y) \oplus key1, & B(x, y) = 3, \\ f(x, y) \oplus \overline{key1}, & B(x, y) = 2, \\ f(x, y) \oplus key2, & B(x, y) = 1, \\ f(x, y) \oplus \overline{key2}, & B(x, y) = 0. \end{cases} \quad (3)$$

2.1.4 Decryption

The decryption procedure is like that of the encryption, since \oplus is an involutive operation².

2.1.5 A constraint

Because not all values of $key1$ and $key2$ can make well-disorderly cipher-images, it is required that $key1$ and $key2$ have 4 different bits (a half of all). In fact, this constraint ensures that the encryption results of $key1$ and $key2$ are sufficiently far.

In [28], CKBA was cryptanalyzed and the following facts were pointed out:

- the security of CKBA against the brute-force attack was over-estimated;
- CKBA is not secure against known/chosen-plaintext attacks, since only one known/chosen plain-image is enough to get an equivalent key, a mask image f_m , by XORing the plain-image f and the cipher-image f' , pixel by pixel: $f_m = f \oplus f'$;
- it is easy to reconstruct the whole secret key $\{key1, key2, x(0)\}$ from the mask image f_m , for which the required complexity is rather small.

² An involutive encryption operation satisfies $f(f(x, k), k) = x$ for any x and k .

Apparently, the insecurity of CKBA against known/chosen-plaintext attacks is determined by the fact that $f(x, y) \oplus f'(x, y)$ is fixed to be one of the four values, $key1$, $\overline{key1}$, $key2$, $\overline{key2}$, at any given position (x, y) . In fact, for any plain-images, f_1, f_2 and their cipher-images, f'_1, f'_2 , one has

$$f_1(x, y) \oplus f'_1(x, y) = f_2(x, y) \oplus f'_2(x, y) \equiv f_m(x, y)$$

for any position (x, y) . As a result, given any cipher-image f' , the plain-image can be decrypted as follows: $f = f' \oplus f_m$.

2.2 RCES [20] (or RSES [19])

RCES is an enhanced version of CKBA, by making $key1$ and $key2$ time-variant, and by introducing a simple permutation operation, $Swap_b(x_1, x_2)$, which exchanges the values of x_1 and x_2 if $b = 1$ and does nothing if $b = 0$.

RCES encrypts plain-images block by block, where each block contains 16 consecutive pixels. To simplify the following description, without loss of generality, assume that the sizes of plain-images are all $M \times N$, and that MN can be divided by 16. Consider a plain-image $\{f(x, y)\}_{x=0, y=0}^{x=M-1, y=N-1}$ as a 1-D pixel-sequence $\{f(l)\}_{l=0}^{MN-1}$ by scanning it line by line from bottom to top. The plain-image can be divided into $MN/16$ blocks:

$$\{f^{(16)}(0), \dots, f^{(16)}(k), \dots, f^{(16)}(MN/16 - 1)\},$$

where

$$f^{(16)}(k) = \{f(16k + 0), \dots, f(16k + i), \dots, f(16k + 15)\}.$$

For the k -th pixel-block $f^{(16)}(k)$, the work mechanism of RCES can be described as follows.

2.2.1 The secret key

The secret key includes the control parameter μ and the initial condition $x(0)$ of the Logistic map (1).

2.2.2 Initialization

Run the Logistic map to generate a chaotic sequence, $\{x(i)\}_{i=0}^{MN/16-1}$, and then extract the 24-bit representation of $x(i)$ to yield a PRBS $\{b(i)\}_{i=0}^{3MN/2-1}$. Note that the Logistic map is realized in 24-bit fixed-point arithmetic.

2.2.3 Encryption

Two pseudo-random seeds,

$$Seed1(k) = \sum_{i=0}^7 b(24k + i) \times 2^{7-i}, \quad (4)$$

$$Seed2(k) = \sum_{i=0}^7 b(24k + 8 + i) \times 2^{7-i}, \quad (5)$$

are calculated to encrypt the current plain-block with the following two steps:

- *Step 1 – Pseudo-randomly swapping adjacent pixels:* for $i = 0 \sim 7$, do

$$Swap_{b(24k+16+i)}(f(16k + 2i), f(16k + 2i + 1)). \quad (6)$$

- *Step 2 – Masking the current plain-block with the two pseudo-random seeds:* for $j = 0 \sim 15$, do

$$f'(16k + j) = f(16k + j) \oplus Seed(16k + j), \quad (7)$$

where

$$Seed(16k + j) = \begin{cases} Seed1(k), & B(k, j) = 3, \\ Seed1(k), & B(k, j) = 2, \\ Seed2(k), & B(k, j) = 1, \\ Seed2(k), & B(k, j) = 0, \end{cases} \quad (8)$$

and $B(k, j) = 2 \times b(24k + j) + b(24k + j + 1)$.

2.2.4 Decryption

The decryption procedure is similar to the encryption procedure, but the masking operation is exerted before the swapping for each pixel-block.

3 Cryptanalysis of RCES

Although RCES is more complicated than CKBA, as analyzed below, its security is not really enhanced by the introduced design complexity.

In this section, the following results are obtained on the security of RCES: 1) its security against brute-force attack was over-estimated; 2) it is not secure against known/chosen-plaintext attacks, and the number of required plain-images is only $O(1)$ and, in fact, only one or two; 3) there are two available

known/chosen-plaintext attacks, and they can be further combined to make a nearly-perfect attack to RCES; 4) the chosen-plaintext attacks can even achieve much better breaking performance than their known-plaintext versions.

3.1 The Brute-Force Attack

In [19,20], Chen and Yen claimed that the complexity of RCES against brute-force attack is $O(2^{3MN/2})$ since $\{b(i)\}_{i=0}^{3MN/2-1}$ has $3MN/2$ bits. However, such a statement is not true due to the following reason: all $3MN/2$ bits are uniquely determined by the control parameter μ and the initial condition $x(0)$ of the Logistic map (1), which has only 48 secret bits. This means that the key entropy of RCES is only 48. Considering not all values of μ can produce chaoticity in the Logistic map, the key entropy should be even smaller than 48. To simplify the following analysis, assume that the key entropy is $K_\mu < 48$, so the total number of all possible keys for brute-force search is only 2^{K_μ} .

Considering that the complexity of RCES is $O(MN)$ [20, Sec. 2.4], the complexity against the brute-force attack will be $O(2^{K_\mu} \cdot MN)$. Assume $K_\mu = 48$, for a typical image whose size is 256×256 , the complexity is about $O(2^{64})$, which is much smaller than $O(2^{3MN/2}) = O(2^{98304})$, the claimed complexity in [19, 20]. Apparently, the security of RCES against the brute-force attack was over-estimated too much.

Note that one has to find a way to automatically verify the guessed keys, in the case that the attacker does not know any plain-image. This can be done by calculating the distribution of the differences of adjacent pixels. For a wrong key, the obtained image is generally chaotic-like, and the distribution of the pixel-value difference would be nearly uniform. For the correct key, a natural image will be output, which corresponds to a Laplacian distribution of the neighboring differences. Note that the complexity of such a verification process is also $O(MN)$.

3.2 Known-Plaintext Attack 1: Breaking RCES with a Mask Image f_m

Although different seeds are used for pixels at different positions and pseudo-random swapping operations are exerted on the plain-image before masking, the known-plaintext attack breaking CKBA can be efficiently extended to break RCES. With only one known plain-image and its corresponding cipher-image, it is very easy to get a mask image f_m , which can be used as an equivalent key of the secret key $(\mu, x(0))$ to decrypt any cipher-image whose

size is not larger than the size of f_m . When two or more plain-images are known, a swapping matrix Q can be constructed to enhance the breaking performance of the mask image f_m .

3.2.1 Get f_m from One Known Plain-Image

Assume that an $M \times N$ plain-image f_K and its corresponding cipher-image f'_K have been known to an attacker. Similar to the way to get the mask image in the known-plaintext attack to CKBA, the attacker here can get f_m by simply XORing the plain-image and the cipher-image pixel by pixel: $f_m(l) = f_K(l) \oplus f'_K(l)$, where $l = 0 \sim MN - 1$.

With the mask image f_m , the attacker tries to recover the plain-image by XORing the mask image and the cipher-image pixel by pixel: $f(l) = f'(l) \oplus f_m(l)$. If a pixel $f(l)$ is not swapped, $f(l) = f'(l) \oplus f_m(l)$ holds; otherwise, $f(l) = f'(l) \oplus f_m(l)$ is generally not true. Assume that the bit $b(24k + 16 + i)$ in Eq. (6) satisfies the balanced distribution³ over $\{0, 1\}$, it is expected that about half of all plain-pixels are not swapped and can be successfully decrypted with $f_m \oplus f'$. Intuitively, half of plain-pixels should be enough to reveal the main content and some details of the plain-image.

With the secret key $(\mu, x(0)) = (3.915264, 0.2526438)$, which is randomly chosen with the standard `rand()` function, some experiments are made to show the real performance of the mask image f_m in this attack. One known plain-image f_{Lenna} and its cipher-image f'_{Lenna} are shown in Fig. 1. The mask image $f_m = f_{\text{Lenna}} \oplus f'_{\text{Lenna}}$ is given in Fig. 2. For an unknown plain-image f_{Peppers} (Fig. 3a), the mask image f_m is used to recover it from its cipher-image f'_{Peppers} (Fig. 3b). The recovered plain-image $f^*_{\text{Peppers}} = f_m \oplus f'_{\text{Peppers}}$ and the recovery error $|f^*_{\text{Peppers}} - f_{\text{Peppers}}|$ are shown in Fig. 4a and 4b, respectively. It is surprisingly seen that the decryption performance is much better than expected: most (much more than 50%) pixels are successfully recovered, and almost all subtle details remain.

Although the recovery error $|f^*_{\text{Peppers}} - f_{\text{Peppers}}|$ visually shows that most plain-pixels are exactly recovered, statistical data reveal that 33,834 pixels in $f^*_{\text{Peppers}} - f_{\text{Peppers}}$ are not zero, i.e., about 51.63% of pixels are not exactly recovered. To explain why f_m is so effective to recover most pixels of the plain-image with only half exactly-recovered pixels, consider two pixels in the known plain-image, $f(2i)$, $f(2i + 1)$, and their cipher-pixels, $f'(2i)$, $f'(2i + 1)$, where $i = 0 \sim MN/2 - 1$. Then, the corresponding elements of the two pixels in the mask image f_m will be $f_m(2i) = f(2i) \oplus f'(2i)$ and $f_m(2i + 1) =$

³ Strictly speaking, the Logistic map cannot guarantee the balance of each generated bit, since its variant density function is not uniform [38]. In this paper, without loss of generality, it is taken for granted so as to simplify the theoretical analyses.



Fig. 1. One 256×256 known plain-image, f_{Lenna} , and its cipher-image f'_{Lenna} .

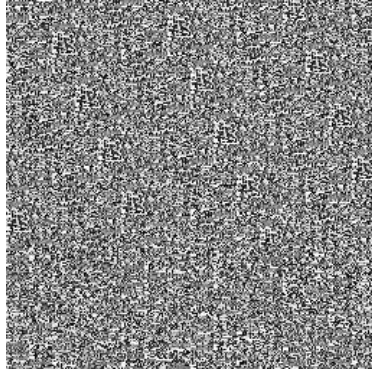


Fig. 2. The mask image f_m derived from f_{Lenna} and f'_{Lenna} .

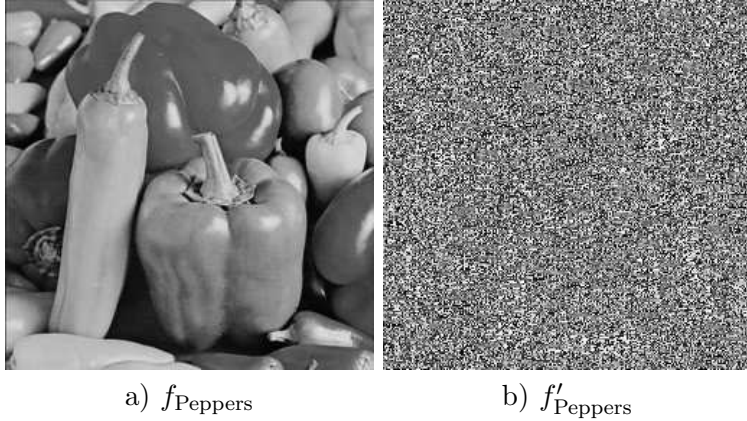


Fig. 3. A 256×256 plain-image unknown to the attacker, f_{Peppers} , and its cipher-image f'_{Peppers} .

$f(2i + 1) \oplus f'(2i + 1)$. Since all recovery errors are introduced at the positions where the adjacent plain-pixels are swapped, one can theoretically study the recovery performance of the mask image f_m by considering the elements corresponding to the swapped pixels only. Assume that $f(2i)$ and $f(2i + 1)$ are swapped in the encryption procedure, $f'(2i) = f(2i + 1) \oplus \text{Seed}(2i)$ and $f'(2i + 1) = f(2i) \oplus \text{Seed}(2i + 1)$. Therefore,

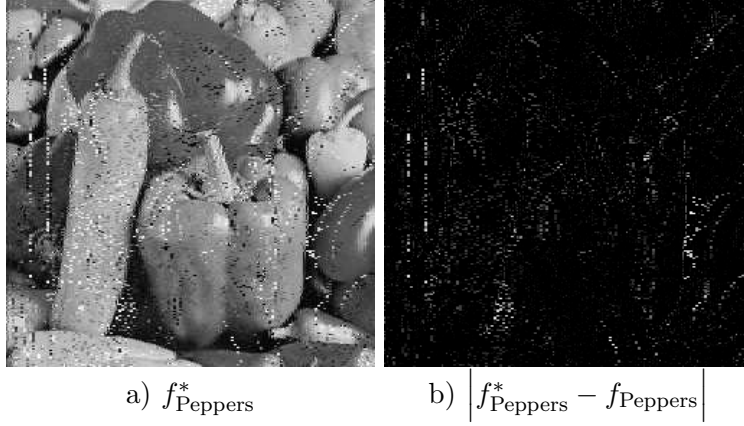


Fig. 4. The result of breaking the plain-image with f_m derived from f_{Lenna} : a) the recovered plain-image $f_{Peppers}^*$; b) the recovery error $|f_{Peppers}^* - f_{Peppers}|$.

$$f_m(2i) = f^{(\oplus)}(2i) \oplus Seed(2i), \quad (9)$$

$$f_m(2i + 1) = f^{(\oplus)}(2i) \oplus Seed(2i + 1), \quad (10)$$

where $f^{(\oplus)}(2i) = f(2i) \oplus f(2i + 1)$.

Consider a cipher-image f'_1 and its corresponding plain-image f_1 . Assuming that the plain-image recovered from f_m is f_1^* , the recovered plain-pixels, $f_1^*(2i)$ and $f_1^*(2i + 1)$, satisfy the following propositions and corollaries. Note that these results are only true for swapped pixels.

Proposition 1 $f_1^*(2i) \oplus f_1(2i) = f_1^*(2i + 1) \oplus f_1(2i + 1) = f^{(\oplus)}(2i) \oplus f_1^{(\oplus)}(2i)$.

Proof: From Eq. (9) and $f'_1(2i) = f_1(2i + 1) \oplus Seed(2i)$,

$$\begin{aligned} f_1^*(2i) &= f_m(2i) \oplus f'_1(2i), \\ &= (f^{(\oplus)}(2i) \oplus Seed(2i)) \\ &\quad \oplus (f_1(2i + 1) \oplus Seed(2i)) \\ &= f^{(\oplus)}(2i) \oplus f_1(2i + 1) \end{aligned}$$

Then, one has

$$\begin{aligned} f_1^*(2i) \oplus f_1(2i) &= f^{(\oplus)}(2i) \oplus f_1(2i + 1) \oplus f_1(2i) \\ &= f^{(\oplus)}(2i) \oplus f_1^{(\oplus)}(2i). \end{aligned}$$

In a similar way, one can get $f_1^*(2i + 1) \oplus f_1(2i + 1) = f^{(\oplus)}(2i) \oplus f_1^{(\oplus)}(2i)$. Thus, the proof is completed. \blacksquare

Corollary 1 When $f(2i) = f(2i + 1)$, $f_1^*(2i) = f_1(2i + 1)$ and $f_1^*(2i + 1) = f_1(2i)$.

Proof: The results of this corollary are special cases of the above two propositions with $f^{(\oplus)}(2i) = 0$. ■

Based on the above propositions, one can get an upper bound of the recovery errors $|f_1^*(2i) - f_1(2i)|$ and $|f_1^*(2i + 1) - f_1(2i + 1)|$. Firstly, a lemma should be introduced.

Lemma 1 *If $a \oplus b = c$, then $|a - b| \leq c$.*

Proof: Represent c in the following binary form:

$$c = (0, \dots, 0, c_{n-1} = 1, \dots, c_i, \dots, c_1, c_0)_2.$$

Similarly, represent a and b as follows:

$$\begin{aligned} a &= (a_{N-1}, \dots, a_{n-1}, \dots, a_i, \dots, a_1, a_0)_2, \\ b &= (b_{N-1}, \dots, b_{n-1}, \dots, b_i, \dots, b_1, b_0)_2. \end{aligned}$$

From $a \oplus b = c$, one have $\forall j = n \sim N - 1, a_j = b_j$. Therefore,

$$\begin{aligned} |a - b| &= \left| \sum_{i=0}^{N-1} (a_i - b_i) \cdot 2^i \right| \\ &= \left| \sum_{i=0}^{n-1} (a_i - b_i) \cdot 2^i \right| \leq \sum_{i=0}^{n-1} |a_i - b_i| \cdot 2^i. \end{aligned}$$

Since $|a_i - b_i| = a_i \oplus b_i = c_i$, one has $|a - b| \leq \sum_{i=0}^{n-1} c_i \cdot 2^i = c$. The lemma is thus proved. ■

Corollary 2 $|f_1^*(2i) - f_1(2i)| \leq f^{(\oplus)}(2i) \oplus f_1^{(\oplus)}(2i)$, and $|f_1^*(2i + 1) - f_1(2i + 1)| \leq f^{(\oplus)}(2i) \oplus f_1^{(\oplus)}(2i)$.

Proof: This corollary is an obvious result of Proposition 1 and Lemma 1. ■

Corollary 2 says that the recovery errors of both $f_1^*(2i)$ and $f_1^*(2i + 1)$ will not be larger than $f^{(\oplus)}(2i) \oplus f_1^{(\oplus)}(2i) = f(2i) \oplus f(2i + 1) \oplus f_1(2i) \oplus f_1(2i + 1)$. Due to the strong correlation between adjacent pixels of digital images, the distribution of the difference between two adjacent pixels is Gaussian-like. As a result, $f^{(\oplus)}(2i)$ will also obeys a (positive) single-side Gaussian-like distribution, which means that the recovery error of each plain-pixel recovered from f_m will also obey a Gaussian-like distribution. The Gaussian-like distribution of recovery errors actually implies that most recovered pixels are close to the real values of the original plain-pixels. Therefore, the surprising recovery performance of f_m shown in Fig. 4 can be naturally explained.

For the plain-image f_{Peppers} , the histograms of some differential images are plotted to verify the above-mentioned theoretical results. Define two $(M - 1) \times N$ differential images $f^{(-)}$ and $f^{(\oplus)}$:

$$f^{(-)}(x, y) = f(x, y) - f(x + 1, y), \quad (11)$$

$$f^{(\oplus)}(x, y) = f(x, y) \oplus f(x + 1, y), \quad (12)$$

where $x = 0 \sim M - 2$, $y = 0 \sim N$. The histograms of the above two differential images of f_{Peppers} are shown in Fig. 5. When $f = f_{\text{Lenna}}$, $f_1 = f_{\text{Peppers}}$, the histograms of $f^{(\oplus)} \oplus f_1^{(\oplus)}$ and $|f_{\text{Peppers}}^* - f_{\text{Peppers}}|$ are shown in Fig. 6. Apparently, Figure 6 agrees with Corollary 2 very well. Note that only the swapped pixels are enumerated for the histogram of $|f_{\text{Peppers}}^* - f_{\text{Peppers}}|$, since the above theoretical analysis on the recovery errors is only focused on the swapped pixels.

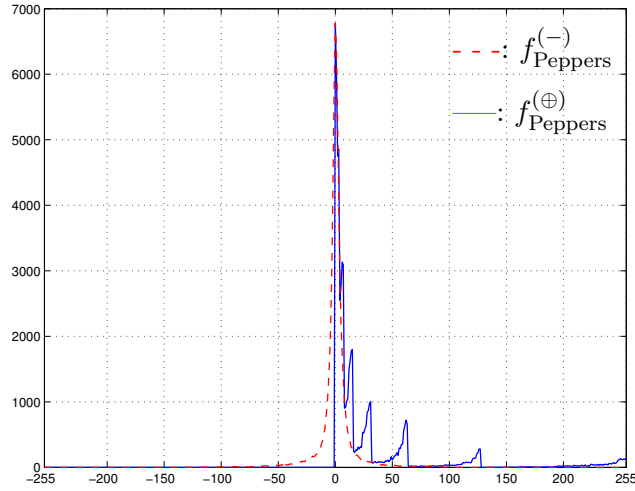


Fig. 5. The histograms of $f_{\text{Peppers}}^{(-)}$ and $f_{\text{Peppers}}^{(\oplus)}$.

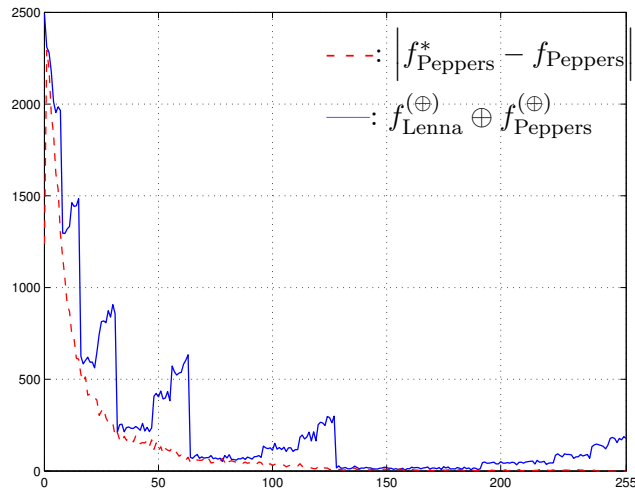


Fig. 6. The histograms of $f_{\text{Lenna}}^{(\oplus)} \oplus f_{\text{Peppers}}^{(\oplus)}$ and $|f_{\text{Peppers}}^* - f_{\text{Peppers}}|$.

Since all recovery errors are introduced by swapped pixels, the recovery performance will be better if some swapped pixels can be distinguished. In the following, it is shown that an attacker can manage to do so by manually detecting visible noises in cipher-images, and by intersecting multiple mask images generated from different known plain-images.

3.2.2 Amending f_m with More Known Cipher-Images

Assume that the corresponding plain-image of a cipher-image does not contain salt-pepper impulsive noises. Then, one can assert that all such noises in the recovered plain-image indicates the positions of swapped pixels. Observing the recovered plain-image f_{Peppers}^* shown in Fig. 4a, one can find many distinguishable noises by naked eyes, which correspond to the strong edges of the known plain-image f_{Peppers} (see Fig. 4b). Following Proposition 1, strong edges means large values of $f^{(\oplus)}(x)$, and so generates salt-pepper noises.

Once some swapped pixels are distinguished, one can generate a swapping $(0, 1)$ -matrix $Q = [q_{i,j}]_{M \times N}$, where $q_{i,j} = 1$ for swapped pixels and $q_{i,j} = 0$ for others. Similarly, Q can be represented in 1-D form: $Q = \{q(l)\}_{l=0}^{MN-1}$. With the swapping matrix, the mask image f_m is amended as follows: for $i = 0 \sim MN/2 - 1$, if $q(2i) = 1$ or $q(2i + 1) = 1$, the values of $f_m(2i)$ and $f_m(2i + 1)$ are re-calculated as follows: $f_m(2i) = f(2i) \oplus f'(2i + 1)$ and $f_m(2i + 1) = f(2i + 1) \oplus f'(2i)$; otherwise, $f_m(2i)$ and $f_m(2i + 1)$ are left untouched. With the amended f_m and the swapping matrix Q , one can decrypt the cipher-images in the following two steps:

- use f_m to XOR the cipher-image to get an initial recovered plain-image f^* ;
- $\forall i = 0 \sim MN/2 - 1$, if $q(2i) = 1$ or $q(2i + 1) = 1$, swap the two adjacent pixels $f^*(2i)$ and $f^*(2i + 1)$.

If an attacker can get more cipher-images encrypted with the same key, he can distinguish more swapped pixels, and gets better recovery performance with f_m and Q . This implies that more and more knowledge on how to purify the attack can be learned from the cipher-images, which is a desirable feature from an attacker's point of view.

3.2.3 Amending f_m with More Known Plain-Images

With two or more known plain-images and their cipher-images encrypted with the same secret key, it is possible to successfully distinguish most swapped pixels, achieving nearly perfect recovery performance. Given $n \geq 2$ known plain-images, f_1, \dots, f_n , and their cipher-images, f'_1, \dots, f'_n , one can get n mask images $f_m^{(i)} = f_i \oplus f'_i$ ($i = 1 \sim n$). Apparently, if the l -th pixel is not swapped, $\forall i \neq j$, $f_m^{(i)}(l) = f_m^{(j)}(l)$. That is, if $f_m^{(i)}(l) \neq f_m^{(j)}(l)$, it can be

asserted that the pixel at this position is swapped. Therefore, by comparing the elements of n mask images, some positions corresponding to the swapped pixels can be distinguished. With the swapping information, following the same way described above, a swapping matrix Q can be constructed, and then f_m is amended with Q with the way mentioned above. Using the amended f_m and the swapping matrix Q , the cipher-image is decrypted with XOR and swapping operations.

From Eqs. (9) and (10), the probability of $f_m^{(i)}(l) \neq f_m^{(j)}(l)$ is the probability of $f_i^{(\oplus)}(2i) \neq f_j^{(\oplus)}(2i)$, where $l = 2i$ or $2i + 1$. Assume the n mask images are independent of each other and the value of each element distributes uniformly over $\{0, \dots, 255\}$. The probability of $f_m^{(i)}(l) \neq f_m^{(j)}(l)$ will be $1 - 256^{-1} \approx 0.996$. This means that only two mask images are enough to distinguish almost all swapped pixels. However, since the mask images are generally not independent of each other and $f_m(l)$ does not obey uniform distribution, the real probability will be less than $1 - 256^{-1}$. Fortunately, for most natural images, this probability is still sufficiently close to $1 - 256^{-1}$, so that two known plain-images are still enough to distinguish most swapped pixels. Given two known plain-images, f_{Lenna} (Fig. 1a) and f_{Barbara} (Fig. 7a), the recovery performance of the attack corresponding to f_{Peppers} is shown in Fig. 7b. It can be seen that the recovered plain-image is almost perfect, and only 952 (about 1.45% of all) pixels are not exactly recovered.

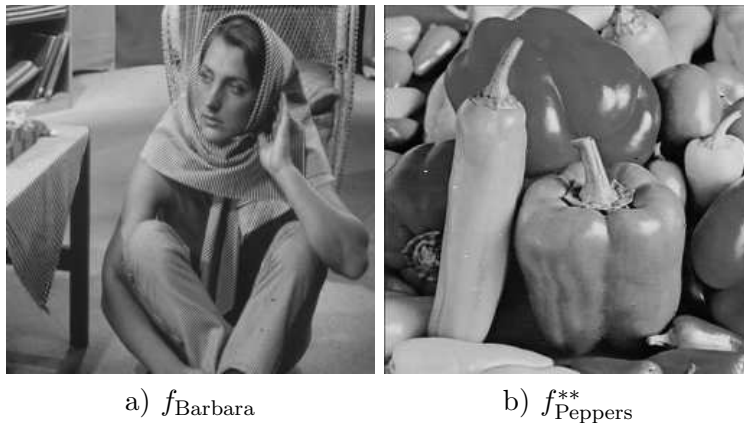


Fig. 7. Another known plain-image f_{Barbara} and the recovered plain-image f_{Peppers}^{**} with two known plain-images: f_{Lenna} and f_{Barbara} .

3.2.4 Enhancing the Recovered Plain-Image with Image Processing Techniques

To further improve the visual quality of the recovered plain-images, some noise reducing techniques can be used to further reduce the recovery errors. For the recovered plain-image f_{Peppers}^* in Fig. 4a, the enhanced plain-image $f_{\text{Peppers}}^{*,3 \times 3}$ with a 3×3 median filter and the corresponding recovery error

$|f_{\text{Peppers}}^{*,3\times3} - f_{\text{Peppers}}|$ are shown in Fig. 8a and 8b, respectively. It can be seen that the visual quality of f_{Peppers}^* is enhanced significantly. Note that more complicated image processing techniques are still available to further polish the recovered plain-image, one of which will be introduced below in Sec. 3.5.

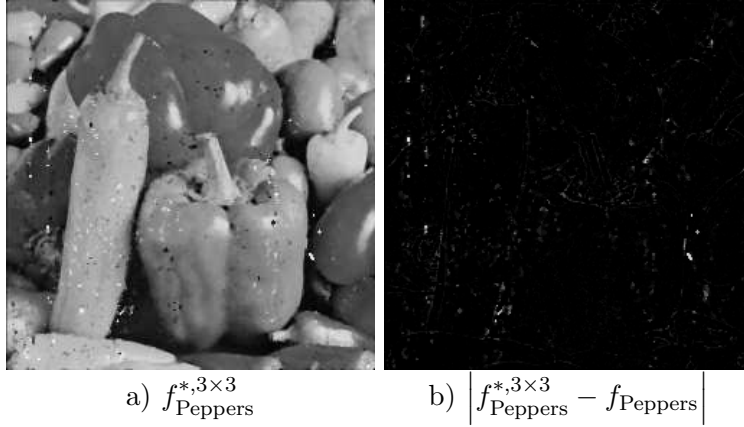


Fig. 8. The result of enhancing the recovered plain-image f_{Peppers}^* with a 3×3 median filter: a) the enhanced image $f_{\text{Peppers}}^{*,3\times3}$; b) the recovery error $|f_{\text{Peppers}}^{*,3\times3} - f_{\text{Peppers}}|$.

3.3 Known-Plaintext Attack 2: Breaking the Chaotic Map

In the above-discussed attack based on mask images, assuming that the size of f_m is $M \times N$, it is obvious that only $M \times N$ leading pixels in a larger cipher-image can be recovered with f_m (and perhaps Q). To decrypt more pixels, the secret control parameter μ and a chaotic state $x(k)$ occurring before $x(MN/16 - 1)$ have to be known, so that one can calculate more chaotic states after $x(MN/16 - 1)$. That is, the chaotic map should be found. Actually, it is possible for an attacker to achieve this goal with a high probability and a sufficiently small complexity, even when only one plain-image is known. Similarly, the more the number of known plain-images are, the closer the probability will be to 1, the smaller the value of k will be, and the lower the attack complexity will be.

3.3.1 Guessing a Chaotic State $x(k)$ from f_m

In the k -th pixel-block, for any unswapped pixel $f(16k + j)$,

$$f_m(16k + j) = f(16k + j) \oplus f'(16k + j) = \text{Seed}(16k + j),$$

which must be one value in the set

$$S_4 = \{ \text{Seed1}(k), \overline{\text{Seed1}(k)}, \text{Seed2}(k), \overline{\text{Seed2}(k)} \}. \quad (13)$$

Therefore, if there are enough unswapped pixels, the right values of $Seed1(k)$ and $Seed2(k)$ can be guessed by enumerating all 2-value and 1-value⁴ combinations of $f_m(16k+0) \sim f_m(16k+15)$. To eliminate most wrong values of $Seed1(k), Seed2(k)$, the following requirements are useful:

- both $B(k, j)$ and $(Seed1(k), Seed2(k))$ are generated with $\{b(24k+j)\}_{j=0}^{15}$;
- $Seed(16k+j)$ is uniquely determined by $B(k, j)$ and $Seed1(k), Seed2(k)$ following Eq. (8).

For each guessed values passing the above requirements, the corresponding chaotic state $x(k) = 0.b(24k+0) \cdots b(24k+23)$ is derived as follows:

- reconstruct $\{b(24k+i)\}_{i=0}^{15}$ from $Seed1(k), Seed2(k)$;
- reconstruct $\{b(24k+16+i)\}_{i=0}^7$ with the following rule: if both $f_m(16k+2i) \in S_4$ and $f_m(16k+2i+1) \in S_4$ hold, $b(24k+16+i) = 0$, else $b(24k+16+i) = 1$.

Note that some extra errors will be introduced in the least 8 bits $\{b(24k+16+i)\}_{i=0}^7$, which makes the derived chaotic state $x(k)$ incorrect. Apparently, the errors are induced by the swapped pixels whose corresponding elements of f_m belong to S_4 . In the following, the probability of such errors, $p_{se} = Prob[f_m(l) \in S_4]$, is studied. For any swapped pixel $f(l)$ in the k -th pixel-block ($l = 16k+0 \sim 16k+15$), according to Eqs. (9) and (10), one has

$$p_{se} = Prob[f^{(\oplus)}(l) \in S_4^{(\oplus)}], \quad (14)$$

where $f^{(\oplus)}(l) = f(2\lfloor l/2 \rfloor) \oplus f(2\lfloor l/2 \rfloor + 1)$ and

$$S_4^{(\oplus)} = \left\{ Seed1(k) \oplus Seed(l), \overline{Seed1(k)} \oplus Seed(l), \right. \\ \left. Seed2(k) \oplus Seed(l), \overline{Seed2(k)} \oplus Seed(l) \right\}.$$

Considering the Gaussian-like distribution of $f^{(\oplus)}$ (see Fig. 5) and the fact that $0 \in S_4^{(\oplus)}$, p_{se} is generally not negligible for natural images. Without loss of generality, assume that each bit in $\{b(i)\}$ yields a balanced distribution over $\{0, 1\}$ and any two bits are independent of each other. One can deduce

$$P_1 = Prob[x(k) \text{ is correct}] = \sum_{i=0}^8 p_b(8, i) \cdot p_c^i, \quad (15)$$

where $p_b(8, i) = \binom{8}{i} \cdot 2^{-8}$, which denotes the probability that there are i pairs of swapped pixels, and $p_c = 1 - p_{se}$. The relation between P_1 and p_c is given in Fig. 9.

⁴ The 1-value combinations are included since $Seed1(k) = Seed2(k)$ may occur with a small probability.

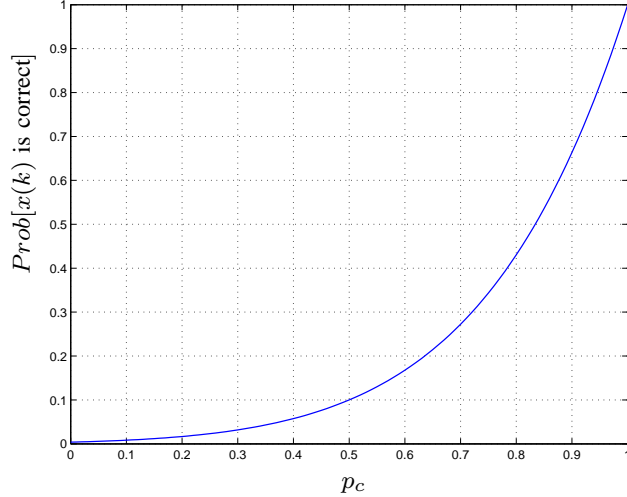


Fig. 9. The relationship between $P_1 = Prob[x(k) \text{ is correct}]$ and p_c .

3.3.2 Deriving μ from Two Consecutive Chaotic States

With two consecutive chaotic states, $x(k)$ and $x(k+1)$, the estimated value of the secret control parameter μ will be $\tilde{\mu}_k = \frac{x(k+1)}{x(k) \cdot (1-x(k))}$. Due to the negative influence of quantization errors, generally $\tilde{\mu}_k \neq \mu$. As known, chaotic maps are sensitive to noise in the initial condition, so an approximate value of μ will generate completely different chaotic states after several iterations, which implies that $\tilde{\mu}_k$ can not be directly used instead of μ as the secret key. Fortunately, if $|\tilde{\mu}_k - \mu|$ is small enough, one can exhaustively search in the neighborhood of $\tilde{\mu}_k$ to find the right value of μ . To verify which guessed value of μ is the right one, one should iterate the Logistic map from $x(k+1)$ until $x(MN/16 - 1)$, and then check whether or not the corresponding elements in f_m match the calculated chaotic states. Once a mismatch occurs, the current guessed value is discarded, and the next guess will be tried. To minimize the verification complexity, one can check only a number of chaotic states sufficiently far from $x(k+1)$ to eliminate most (or even all) wrong values of $\tilde{\mu}_k$, and verify the left few ones by checking all chaotic states from $x(k+2)$ to $x(MN/16 - 1)$.

Now, the concern is when $|\tilde{\mu}_k - \mu|$ will be small enough to make the exhaustive search practical. According to Proposition 2 (see the Appendix for a proof), when $x(k+1) \geq 2^{-n}$, the quantization error of $\tilde{\mu}_k$ is less than $2^{n+3}/2^L$, which means that the size of the neighborhood of $\tilde{\mu}_k$ for exhaustive search is 2^{n+3} . To make the search complexity practically small in real attacks, $x(k+1) \geq 0.5$ is suggested to derive μ , which occurs with probability 0.5.

Proposition 2 Assume that the Logistic map $x(k+1) = \mu \cdot x(k) \cdot (1-x(k))$ is iterated with L -bit fixed-point arithmetic and that $x(k+1) \geq 2^{-n}$, where $1 \leq n \leq L$. Then, the following inequality holds: $|\mu - \tilde{\mu}_k| \leq 2^{n+3}/2^L$, where

$$\tilde{\mu}_k = \frac{x(k+1)}{x(k) \cdot (1-x(k))}.$$

Combining the above analyses, the final complexity of finding two correct consecutive chaotic states, $x(k)$, $x(k+1)$, and the right value of μ , is

$$O\left(\frac{2 \times \left(\binom{16}{2} + \binom{16}{1}\right)}{(0.5 \times P_1)^2} \times 2^{1+3}\right) = O\left(\frac{17408}{P_1^2}\right), \quad (16)$$

which is generally much smaller than the complexity of exhaustively searching all possible keys. As a reference value, when $p_c = 0.7$, the complexity is about $O(2^{17.8}) \ll O(2^{48})$.

3.3.3 A Quick Algorithm to Guess the Two Random Seeds

Following the above-discussed search process, the found correct chaotic states $x(k)$ and $x(k+1)$ will be close to $x(0)$. Considering the occurrence of two consecutive chaotic states larger than 0.5 as a Bernoulli experiment, the mathematical expectation of k will be $\frac{1}{(0.5 \times P_1)^2} = \frac{4}{P_1^2}$ [39]. This means that only tens of known plain-pixels⁵ are enough for an attacker to break the chaotic map, which is a very desired feature for attackers. However, as an obvious disadvantage, the search complexity to guess the two random seeds is somewhat large. In fact, for each pixel-block, one can only test a few number of possible 2-value (and 1-value) combinations, not all. Fortunately, we have another idea to make the search easier: if this pixel-block looks not good for guessing the two random seeds, simply discard it and go to the next pixel-block. Following such an idea, a quicker algorithm can be designed to find the two random seeds. In this quick-search algorithm, the found correct chaotic states $x(k)$ and $x(k+1)$ may be far from $x(0)$, so the size of the mask image has to be much larger than $\frac{4}{P_1^2}$.

The quick-search algorithm is based on the following observation: the more the unswapped pixels there are in the k -th pixel-block, the more elements in $\{f_m(16k+j)\}_{j=0}^{15}$ belong to S_4 . Then, define a new sequence $\{\tilde{f}_m(16k+j)\}_{j=0}^{15}$ accordingly as follows:

$$\tilde{f}_m(16k+j) = \min\left(f_m(16k+j), \overline{f_m(16k+j)}\right). \quad (17)$$

Then, the following is also true: the more the unswapped pixels there are in the k -th pixel-block, the more the number of the values in S_2 will be in

⁵ For example, even a 10×10 “tiny” image is enough.

$\{\tilde{f}_m(16k + j)\}_{j=0}^{15}$, where

$$S_2 = \left\{ \min \left(\text{Seed1}(k), \overline{\text{Seed1}(k)} \right), \min \left(\text{Seed2}(k), \overline{\text{Seed2}(k)} \right) \right\}.$$

Therefore, assuming that there are n_k pairs of unswapped pixels in the k -th pixel-block, the following fact is true: if n_k is sufficiently large, the two most-occurring elements in $\{\tilde{f}_m(16k + j)\}_{j=0}^{15}$ are the two values in S_2 , with a high probability. Then, the question becomes: when can one say that n_k is sufficiently large? In totally 8 pairs of elements, the average number of pairs in S_2 is $N(S_2) = n_k + (8 - n_k) \cdot p_{se}$, and the number of other pairs is $N(\overline{S_2}) = 8 - N(S_2) = (8 - n_k) \cdot (1 - p_{se})$. From a conservative point of view, let $N(\overline{S_2}) < \frac{N(S_2)}{2}$, which ensures that the occurring probability of each element of S_2 is larger than the probability of all other values, with a sufficiently high probability. Solving this inequality, one can get $n_k \geq 6$, yielding $N(\overline{S_2}) \leq 2 < 3 \leq \frac{N(S_2)}{2}$.

Based on the above analyses, the quick-search algorithm is described as follows:

- *Step 1*: for each pixel-block, generate a new sequence, $\{\tilde{f}_m(16k + j)\}_{j=0}^{15}$;
- *Step 2*: rank all values of $\{\tilde{f}_m(16k + j)\}_{j=0}^{15}$ to find the top two mostly-occurring values, *value1* and *value2*;
- *Step 3*: if the occurrence times of *value1* and *value2* is not less than 12, or if the occurrence times of *value2* is less than 3, skip the current pixel-block and goto *Step 1*;
- *Step 4*: in the set $\tilde{S}_4 = \{\text{value1}, \overline{\text{value1}}, \text{value2}, \overline{\text{value2}}\}$, exhaustively search *Seed1*(k) and *Seed2*(k).

If more than one value corresponds to the same position in the rank of $\{\tilde{f}_m(16k + j)\}_{j=0}^{15}$, all of them should be enumerated as *value1* and *value2* in Step 2 to Step 4. In a real attack, some extra constraints, such as the relation between the random seeds and $B(k, j)$ (which is due to the reuse of some chaotic bits), can be added to further optimize the above algorithm for different mask images. The attack complexity of this quick-search algorithm is hard to theoretically analyzed, since the distribution of those values that are not in S_4 is generally unknown. Fortunately, experiments show that the complexity is much smaller than the one given above. In Fig. 10, the performance of the quick-search algorithm is shown for the recovered plain-image f_{Peppers}^* , where different pixel-blocks are used to extract the chaotic states. Note that more than forty pixel-blocks are eligible to be used to extract the correct chaotic states, and the three shown here are randomly chosen for demonstration.

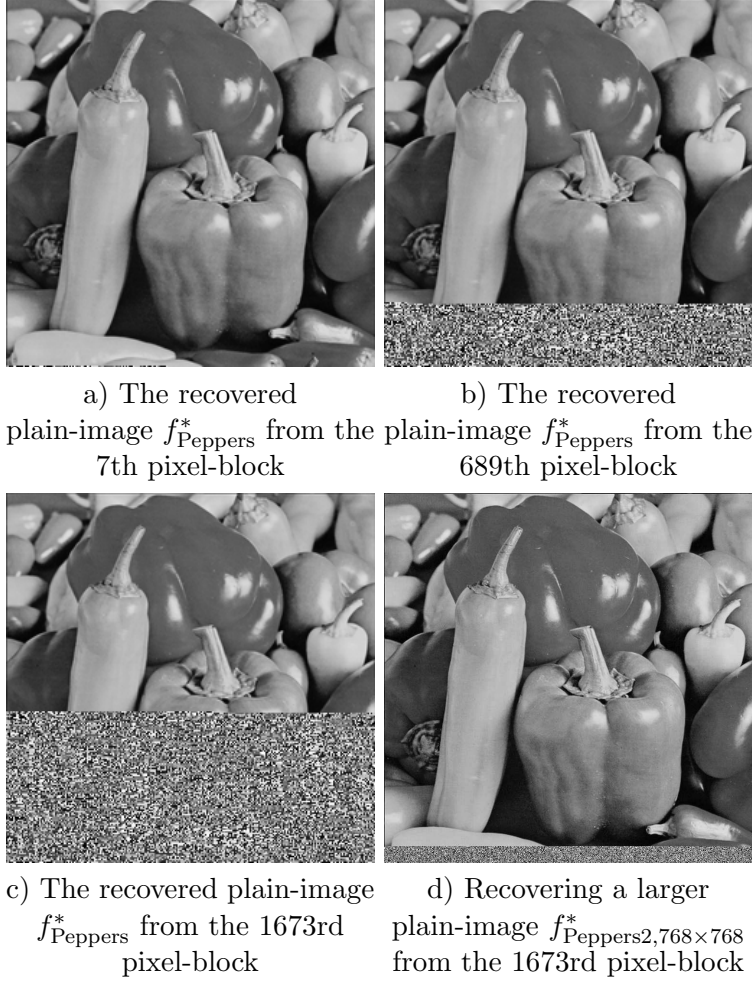


Fig. 10. Demonstration of the quick-search algorithm, where f_{Lenna} is the only known plain-image.

In the following, it is theoretically studied as how much MN should be to guarantee the efficiency of the quick-search algorithm, which is determined by the occurrence probability that two consecutive pixel-blocks satisfy the requirements given in Step 1 and Step 3. Assume that each bit in $\{b(i)\}$ yields a balanced distribution over $\{0, 1\}$ and any two bits are independent of each other. The probability that one pixel-block satisfies the requirements, which is denoted by P_o , yields Eq. (18). Then, for the occurrence probability that two consecutive pixel-blocks satisfy the requirements, which is denoted by P_{o2} , one can calculate that $P_{o2} = P_o^2 \geq \text{Prob} [S_4 = \tilde{S}_4]^2 = \left(\frac{4699}{2^{15}}\right)^2 \approx 0.02$. This means that there will be two consecutive pixel-blocks satisfy the requirements in $\frac{1}{P_{o2}} \approx 50$ pixel-blocks (about 800 pixels), from the probabilistic point of view. Therefore, the required size of the known plain-image should be larger than 800, which is even smaller than the size of a 30×30 image. Hence, the quick-search algorithm is very efficient to use for attacks.

$$\begin{aligned}
P_o &\geq \text{Prob} [S_4 = \tilde{S}_4] \\
&= \text{Prob} \left[\text{both } \text{Seed1}(k) \text{ and } \text{Seed2}(k) \text{ occur } \geq 3 \text{ times in } \left\{ \tilde{f}_m(16k + j) \right\}_{j=0}^{15} \right] \\
&\quad \cdot \text{Prob} \left[\min \left(\text{Seed1}(k), \overline{\text{Seed1}(k)} \right) \neq \min \left(\text{Seed2}(k), \overline{\text{Seed2}(k)} \right) \right] \\
&= \sum_{n_k=6}^8 \left(\binom{8}{n_k} \cdot 2^{-8} \cdot \left(1 - \sum_{m=0}^2 \binom{2n_k}{m} \cdot 2^{-2n_k} \right) \cdot (1 - 128^{-1}) \right) \tag{18}
\end{aligned}$$

3.3.4 Breaking the Chaotic Map with both f_m and Q

All the above-mentioned algorithms are based on only-one known plain-image. When more than one plain/cipher-image is known, the constructed swapping (0,1)-matrix Q will be very useful to increase the efficiency of the attack. As already known, the mask image f_m can be amended using the swapping information stored in Q . Since all amended elements in f_m are also values in S_4 , it is obvious that the efficiency of the search algorithm for finding correct random seeds will be increased. In addition, the swapping matrix Q can be used to uniquely determine some bits in $\{b(24k + 16 + i)\}_{i=0}^7$ without checking $f_m(16k + 2i) \in S_4$ and $f_m(16k + 2i + 1) \in S_4$. Thus, the total complexity in finding a correct chaotic state will be less, and the attack will succeed faster.

When two or more plain-images and/or cipher-images are known, most swapped pixels can be successfully distinguished. In this case, it is much easier to find a pixel-block of f_m whose elements are all in S_4 , which means that $\text{Seed1}(k)$, $\text{Seed2}(k)$ can be quickly guessed by enumerating all values in S_4 , and all the 8 bits $\{b(24k + 16 + i)\}_{i=0}^7$ can be absolutely determined. This implies that the attack complexity is minimized to be the complexity of breaking RCES's weaker parent – CKBA [28].

3.4 The Combined Known-Plaintext Attack

The above two known-plaintext attacks have their disadvantages: the first attack cannot decrypt the cipher-images larger than MN (the size of f_m), and the second one cannot decrypt all pixels before the position where the first correct chaotic state $x(k)$ is found. One can combine them, however, to make a better known-plaintext attack without these disadvantages: use the first attack to decrypt the pixels before $x(k)$ and then use the second attack to decrypt the others. Figure 11 shows the performance of this combined attack with only one known plain-image, where the recovered chaotic state in the second attack is selected as $x(1673)$ (see also Fig. 10c), which can clearly show the boundary of the two parts decrypted by the two attacks.



a) The recovered plain-image f_{Peppers}^*

b) The recovered larger plain-image $f_{\text{Peppers}2,768 \times 768}^*$

Fig. 11. The recovery performance of the combined known-plaintext attack.

3.5 The Chosen-Plaintext Attack

Apparently, all the above three known-plaintext attacks can be extended to chosen-plaintext attacks.

For the first kind of known-plaintext attack, the chosen-plaintext version can achieve much better recovery performance with a nearly-perfect mask image f_m , by choosing only one plain-image whose pixels are all fixed to be the same gray value. Given such a plain-image, from Corollary 1, any recovered plain-pixel will be the plain-pixel itself or its adjacent pixel. Thus, although the recovery error bounded by $a_1 = f_1(16k + 2i) \oplus f_1(16k + 2i + 1)$ may still be large, it is expected that the visual quality of the recovered plain-image will be much better. It is also expected that all salt-pepper impulsive noises will disappear and a dithering effect of edges will occur, which is demonstrated in Fig. 12c with the plain-image f_{Peppers}^* recovered from the chosen plain-image shown in Fig. 12a. As a natural result, the visual quality of the recovered plain-image f_{Peppers}^* becomes much better as compared with the one shown in Fig. 4a.

Similarly to the known-plaintext attack, with some image processing techniques, the recovered plain-image in the chosen-plaintext attack can also be enhanced to further provide a better visual quality. Now, the question is: can one maximize the visual quality with an optimization algorithm? The answer is yes. In fact, with a subtly-designed algorithm, almost all dithering edges can be perfectly polished and a matrix Q containing partial swapping information can be constructed with only one chosen plain-image. In the following, this efficient algorithm and its real performance are studied in detail.

The proposed algorithm divides the image into $2n$ -pixel blocks for enhancement, where $2n$ can exactly divide M . The basic idea is to exhaustively search the optimal swapping states of all pixels to achieve the minimal differential

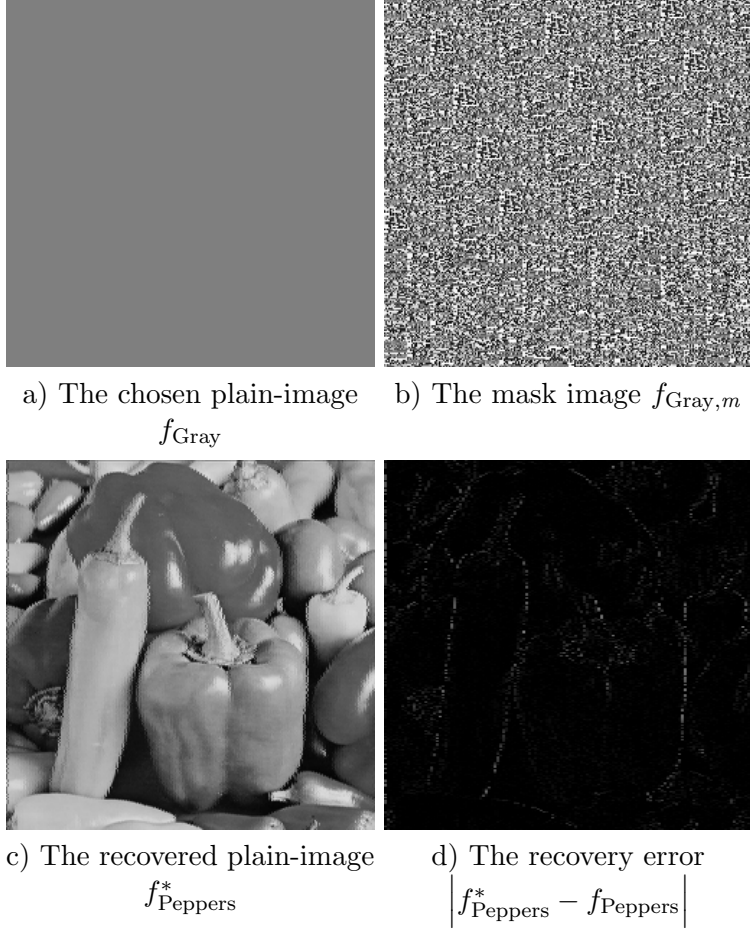


Fig. 12. The recovery performance of the chosen-plaintext attack.

errors. For the m -th $2n$ -pixel block $f_B(m) = \{f(m \cdot 2n + i)\}_{i=0}^{2n-1}$, the algorithm works as follows:

- (1) set $\{b_s(i) = 0\}_{i=0}^{n-1}$ and $\Delta_{\min} = 256(n - 1)$;
- (2) for $(b_0, \dots, b_{n-1}) = (\overbrace{0, \dots, 0}^n) \sim (\overbrace{1, \dots, 1}^n)$, do
 - (a) assign $A = \{a_0, \dots, a_{2n-1}\} = f_B(m)$;
 - (b) for $i = 0 \sim n - 1$, do $\text{Swap}_{b_i}(a_{2i}, a_{2i+1})$;
 - (c) calculate $\Delta A = |a_2 - a_1| + |a_4 - a_3| + \dots + |a_{2i} - a_{2i-1}| + \dots + |a_{2n-2} - a_{2n-3}|$;
 - (d) if $\Delta A < \Delta_{\min}$, then set $\Delta_{\min} = \Delta A$ and $\{b_s(i) = b_i\}_{i=0}^{n-1}$.
- (3) for $i = 0 \sim n - 1$, do $\text{Swap}_{b_s(i)}(f(m \cdot 2n + 2i), f(m \cdot 2n + 2i + 1))$;
- (4) set the corresponding elements of the swapping matrix Q to be 1 for $b_s(i) = 1$.

The complexity of the above algorithm is $O(2^n \cdot MN)$. When $M = N = 256$ and $n = 8$, it is less than 2^{24} , which is practical even on PCs.

For the recovered plain-image f_{Peppers}^* shown in Fig. 12c, the above algorithm

has been tested with parameter $n = 8$, and the result is given in Figs. 13a and 13b. Although the enhanced plain-image have 14378 (about 21.94% of all) pixels different from the original plain-image, its visual quality is so perfect that no any visual degradation can be distinguished. In fact, in a sense, the enhanced plain-image can be considered as a better version of the original one, since each $2n$ -pixel block of the former reaches the minimum of the accumulated differential error. From such a point of view, this optimization algorithm can also be used to enhance the visual quality of the plain-image recovered by a known-plaintext attack. For the recovered plain-image shown in Fig. 4a, the enhancing result is given in Figs. 13c and 13d. It can be seen that dithering edges existing in the plain-image shown in Fig. 4a have been polished.

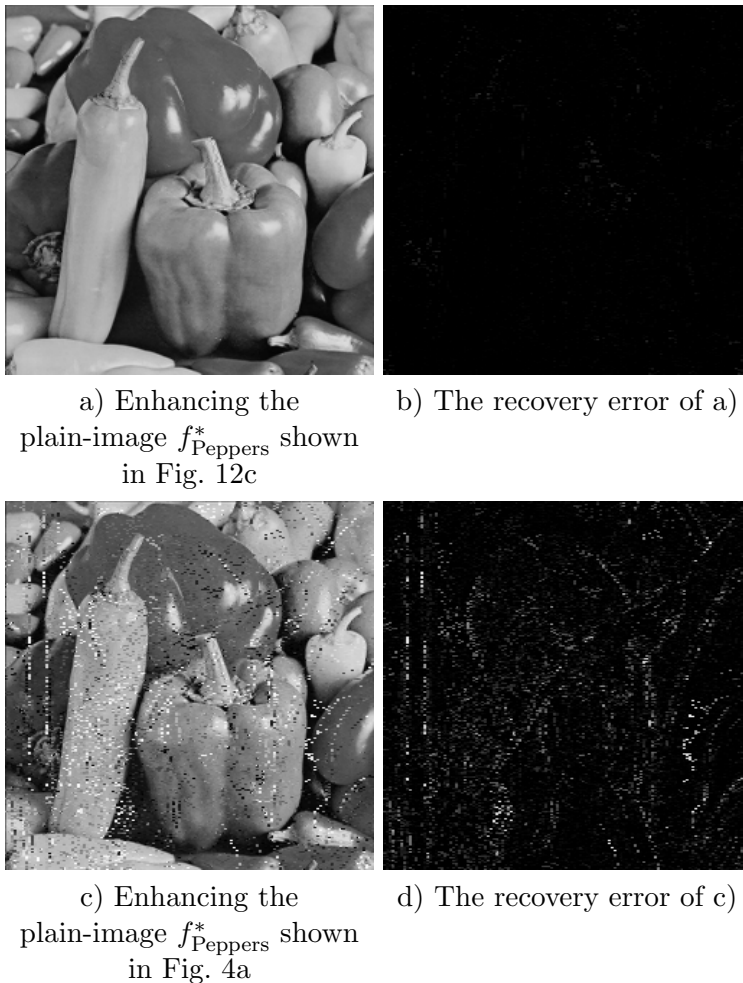


Fig. 13. The performance of the optimization algorithm discussed in Sec. 3.5, when $n = 8$.

In the above algorithm, most swapped operations can be distinguished by using the minimum-detecting rule on the accumulated differential error of $f_B(m)$, which means that most elements in Q are correct for showing the real values of the swapping directive bits $\{b(24k + 16 + i)\}_{i=0}^7$. Once 32 consecutive correct elements (two 16-pixel blocks) in Q have been found, it is possible to

derive μ and a chaotic state $x(k)$, like in the situation of the second known-plaintext attack.

4 Lessons Learned from RCES/CKBA

From the above cryptanalysis of RCES, some principles can be suggested for the design of good image encryption schemes. Although the security of RCES and CKBA against the known/chosen-plaintext attack is very weak, they are still useful as typical carelessly-designed examples to show what one should do and what one should not do⁶.

4.1 Principle 1: Security against the known/chosen-plaintext attacks should be provided

As surveyed in [36], besides CKBA/RCES, many other image encryption schemes are also insecure against the known/chosen-plaintext attack. However, without the capability against the known/chosen-plaintext attacks, it will be insecure to repeatedly use the same secret key to encrypt multiple image files. When the cryptosystems are used to encrypt image streams transmitted over networks, this problem can be relaxed due to the use of time-variant session keys [40]. Considering that most image encryption systems are proposed to encrypt local image files, the security against the known/chosen-plaintext attacks is generally required.

4.2 Principle 2: Do not use invertible encryption function

Rewrite the encryption function of a symmetric cipher as $C = E(P, K)$. The function $E(\cdot, \cdot)$ is said to be invertible, if K can be derived from C and P with its inverse function $E^{-1}(\cdot, \cdot)$, i.e., $K = E^{-1}(P, C)$. Most modern ciphers employ a mixture of operations defined in different groups to make the encryption function non-invertible.

In RCES/CKBA, the encryption function is XOR, which is an invertible operation since $P \oplus K = C \Rightarrow K = P \oplus C$. It is the essential reason why the mask image f_m can be used as an equivalent of the real key $(x(0), \mu)$. Similarly, the invertibility of the swapping operations is the reason for the success of the dithering-removal algorithm discussed in the chosen-plaintext attack.

⁶ For more discussions on how to design a good image encryption schemes, see Sec. 4.5 of [36].

To enhance the security of RCES, the XOR operation can be replaced with some key-dependent invertible functions. Another way is to replace the swapping operation with more complex long-distance permutation operations, such as the ones used in [8–11]. If both operations are changed as above, the security will be further enhanced. References [8–11] suggest some typical image ciphers that use such an idea to ensure the security against the known/chosen-plaintext attacks.

4.3 Principle 3: The correlation information within the plain-image should be sufficiently reduced

As shown in the previous section, the high correlation information between adjacent pixels is an important reason of the good performances for the known/chosen-plaintext attacks. In fact, there exists a large amount of correlation information within digital images, even between pixels whose distances are large, such as pixels in a smooth area. To provide sufficient security against attacks, the correlation information within the plain-image should be sufficiently concealed. A typical method to conceal the correlation information is to carry out complex long-distance permutation operations [8–11]. Note that the long-distance permutations are not necessary conditions, but sufficient ones, since any secure text cipher can also provide enough security for digital images.

4.4 Principle 4: Any non-uniformity existing in the cipher-images should be avoided

From a cryptographer’s point of view, any non-uniformity is not welcome due to the risk of causing statistics-based attacks, such as the well-known differential attacks [40]. So, it should be carefully checked whether or not there exists any non-uniformity in the ciphertexts.

The essential reason for the insecurity of RCES/CKBA against the known/chosen-plaintext attacks can also be ascribed to the non-uniformity of the distribution of $f(l) \oplus f'(l)$ over $\{0, \dots, 255\}$:

- for any unswapped pixel, $Prob[f(l) \oplus f'(l) = Seed(l)] = 1$, i.e., the distribution is one with the most non-uniformity;
- for any swapped pixel, the distribution of $f(l) \oplus f'(l)$ has the same non-uniformity level as the one of $f(l) \oplus f(l+1)$ (see the distribution of $f_{Peppers}^{(\oplus)}$ shown in Fig. 5).

This also suggests that all pixels should be permuted. Actually, in the second known-plaintext attack, the feasibility of the quick-search algorithm in finding

the two random seeds is benefited from the non-uniformity of the distribution of $\{\tilde{f}_m(16k + j)\}_{j=0}^{15}$ over the discrete set $\{0, \dots, 127\}$. If each $\tilde{f}_m(16k + j)$ distributes uniformly over $\{0, \dots, 127\}$, the exhaustive search algorithm will be practically impossible when the block size is changed to a sufficiently large value.

5 Conclusion

In this paper, it has been pointed out that the RCES/RSES image encryption method recently proposed in [19, 20] is not secure enough against the known/chosen-plaintext attacks, and that the security against brute-force attack was overestimated. Both theoretical and experimental analyses have been given to support the feasibility of the known/chosen-plaintext attacks. The insecurity of RCES are caused by a careless design, and some principles on good design of secure image encryption schemes can be learned from the weakness of RCES. In summary, although RCES cannot be used in practice as a secure cipher to protect digital images, it provides a typical example for caution.

Acknowledgements

Shujun Li was sponsored by the Alexander von Humboldt Foundation, Germany. The work of K.-T. Lo was supported by the Research Grants Council of the Hong Kong SAR Government under Project Number 523206 (PolyU 5232/06E).

Appendix

Here we give the proof of Proposition 2, which has occurred in Page 423 of [41] (but with different notations).

Proposition 2 *Assume that the Logistic map $x(k+1) = \mu \cdot x(k) \cdot (1 - x(k))$ is iterated with L -bit fixed-point arithmetic and that $x(k+1) \geq 2^{-n}$, where $1 \leq n \leq L$. Then, the following inequality holds: $|\mu - \tilde{\mu}_k| \leq 2^{n+3}/2^L$, where $\tilde{\mu}_k = \frac{x(k+1)}{x(k) \cdot (1 - x(k))}$.*

Proof: In L -bit fixed-point arithmetic, μ , $x(k)$, and $x(k+1)$ all have L binary decimal bits, and the quantization error of $x(k+1)$ can be explained in the

following equation:

$$\begin{aligned} x(k+1) &= (\mu \cdot x(k) + e'_{x(k+1)}) \cdot (1 - x(k)) + e''_{x(k+1)} \\ &= \mu \cdot x(k) \cdot (1 - x(k)) + e_{x(k+1)}, \end{aligned}$$

where $|e_{x(k+1)}| = |e'_{x(k+1)} \cdot (1 - x(k)) + e''_{x(k+1)}| \leq |e'_{x(k+1)}| + |e''_{x(k+1)}|$. Considering $|e'_{x(k+1)}|, |e''_{x(k+1)}| < 2^{-L}$ for floor/ceil quantization functions and $|e'_{x(k+1)}|, |e''_{x(k+1)}| \leq 2^{-(L+1)}$ for the round function, $|e_{x(k+1)}| < 2^{-(L-1)}$ is true in all cases. Then, the quantization error $|e_{\mu_k}^{\sim}| = |\mu - \tilde{\mu}_k|$ can be estimated as follows:

$$\begin{aligned} |e_{\mu_k}^{\sim}| &= \left| \frac{x(k+1) + e_{x(k+1)}}{x(k) \cdot (1 - x(k))} - \frac{x(k+1)}{x(k) \cdot (1 - x(k))} \right| \\ &= \left| \frac{e_{x(k+1)}}{x(k+1)} \cdot \frac{x(k+1)}{x(k) \cdot (1 - x(k))} \right| = \frac{|e_{x(k+1)}|}{x(k+1)} \cdot \mu \\ &< \frac{2^{-(L-1)} \cdot \mu}{x(k+1)} \leq \frac{4}{2^{L-1} \cdot x(k+1)} = \frac{1}{2^{L-3} \cdot x(k+1)}. \end{aligned}$$

When $x(k+1) \geq 2^{-n}$ ($n = 1 \sim L$),

$$|e_{\mu_k}^{\sim}| < \frac{1}{2^{L-3} \cdot x(k+1)} \leq \frac{2^n}{2^{L-3}} = 2^{n+3}/2^L. \quad (19)$$

This finishes the proof of the proposition. ■

References

- [1] P. P. Dang, P. M. Chau, Image encryption for secure internet multimedia applications, *IEEE Trans. Consumer Electronics* 46 (3) (2000) 395–403.
- [2] N. G. Bourbakis, C. Alexopoulos, Picture data encryption using SCAN patterns, *Pattern Recognition* 25 (6) (1992) 567–581.
- [3] C. Alexopoulos, N. G. Bourbakis, N. Ioannou, Image encryption method using a class of fractals, *J. Electronic Imaging* 4 (3) (1995) 251–259.
- [4] K.-L. Chung, L.-C. Chang, Large encryption binary images with higher security, *Pattern Recognition Letters* 19 (5–6) (1998) 461–468.
- [5] H. Cheng, X. Li, Partial encryption of compressed images and videos, *IEEE Trans. Signal Processing* 48 (8) (2000) 2439–2451.

- [6] C.-C. Chang, M.-S. Hwang, T.-S. Chen, A new encryption algorithm for image cryptosystems, *J. Systems and Software* 58 (2) (2001) 83–91.
- [7] A. Pommer, Selective encryption of wavelet-compressed visual data, Ph.D. thesis, Department of Scientific Computing, University of Salzburg, Austria (June 2003).
- [8] S. S. Maniccam, N. G. Bourbakis, Image and video encryption using SCAN patterns, *Pattern Recognition* 37 (4) (2004) 725–737.
- [9] J. Scharinger, Fast encryption of image data using chaotic Kolmogorov flows, *J. Electronic Imaging* 7 (2) (1998) 318–325.
- [10] J. Fridrich, Symmetric ciphers based on two-dimensional chaotic maps, *Int. J. Bifurcation and Chaos* 8 (6) (1998) 1259–1284.
- [11] Y. Mao, G. Chen, S. Lian, A novel fast image encryption scheme based on 3D chaotic Baker maps, *Int. J. Bifurcation and Chaos* 14 (10) (2004) 3613–3624.
- [12] K. Yano, K. Tanaka, Image encryption scheme based on a truncated Baker transformation, *IEICE Trans. Fundamentals* E85-A (9) (2002) 2025–2035.
- [13] B. Bhargava, C. Shi, S.-Y. Wang, MPEG video encryption algorithms, *Multimedia Tools and Applications* 24 (1) (2004) 57–79.
- [14] C.-P. Wu, C.-C. J. Kuo, Design of integrated multimedia compression and encryption systems, *IEEE Trans. Multimedia* 7 (5) (2005) 828–839.
- [15] Y. Mao, M. Wu, A joint signal processing and cryptographic approach to multimedia encryption, *IEEE Trans. Image Processing* 15 (7) (2006) 2061–2075.
- [16] J.-C. Yen, J.-I. Guo, A new image encryption algorithm and its VLSI architecture, in: *Proc. IEEE Workshop Signal Processing Systems, 1999*, pp. 430–437.
- [17] J.-C. Yen, J.-I. Guo, Efficient hierarchical chaotic image encryption algorithm and its VLSI realisation, *IEE Proc. – Vis. Image Signal Process.* 147 (2) (2000) 167–175.
- [18] J.-C. Yen, J.-I. Guo, A new chaotic key-based design for image encryption and decryption, in: *Proc. IEEE Int. Symposium on Circuits and Systems (ISCAS'2000)*, Vol. 4, 2000, pp. 49–52.
- [19] H.-C. Chen, J.-C. Yen, J.-I. Guo, Design of a new cryptography system, in: *Proc. PCM'2002*, Vol. 2532 of *Lecture Notes in Computer Science*, Springer-Verlag, Berlin, 2002, pp. 1041–1048.
- [20] H.-C. Chen, J.-C. Yen, A new cryptography system and its VLSI realization, *J. Systems Architecture* 49 (7-9) (2003) 355–367.
- [21] H.-C. Chen, J.-I. Guo, L.-C. Huang, J.-C. Yen, Design and realization of a new signal security system for multimedia data transmission, *EURASIP J. Applied Signal Processing* 2003 (13) (2003) 1291–1305.

- [22] J.-C. Yen, J.-I. Guo, The design and realization of a new domino signal security system, *Journal of the Chinese Institute of Electrical Engineering (Transactions of the Chinese Institute of Engineers, Series E)* 10 (1) (2003) 69–76.
- [23] J.-K. Jan, Y.-M. Tseng, On the security of image encryption method, *Information Processing Letters* 60 (5) (1996) 261–265.
- [24] L. Qiao, Multimedia security and copyright protection, Ph.D. thesis, Department of Computer Science, University of Illinois at Urbana-Champaign, Urbana, Illinois, USA (1998).
- [25] H. C. H. Cheng, Partial encryption for image and video communication, Master’s thesis, Department of Computing Science, University of Alberta, Edmonton, Alberta, Canada (Fall 1998).
- [26] C.-C. Chang, T.-X. Yu, Cryptanalysis of an encryption scheme for binary images, *Pattern Recognition Letters* 23 (14) (2002) 1847–1852.
- [27] S. Li, X. Zheng, On the security of an image encryption method, in: *Proc. IEEE Int. Conference on Image Processing (ICIP’2002)*, Vol. 2, 2002, pp. 925–928.
- [28] S. Li, X. Zheng, Cryptanalysis of a chaotic image encryption method, in: *Proc. IEEE Int. Symposium on Circuits and Systems (ISCAS’2002)*, Vol. II, 2002, pp. 708–711.
- [29] S. Li, C. Li, G. Chen, N. G. Bourbakis, K.-T. Lo, A general cryptanalysis of permutation-only multimedia encryption algorithms, *IACR’s Cryptology ePrint Archive: Report 2004/374*, available at <http://eprint.iacr.org/2004/374> (2007).
- [30] C. Li, S. Li, G. Chen, G. Chen, L. Hu, Cryptanalysis of a new signal security system for multimedia data transmission, *EURASIP J. Applied Signal Processing* 2005 (8) (2005) 1277–1288.
- [31] C. D. Cannière, J. Lano, B. Preneel, Cryptanalysis of the two-dimensional circulation encryption algorithm, *EURASIP J. Applied Signal Processing* 2005 (12) (2005) 1923–1927.
- [32] C. Li, S. Li, D.-C. Lou, D. Zhang, On the security of the Yen-Guo’s domino signal encryption algorithm (DSEA), *Journal of Systems and Software* 79 (2) (2006) 253–258.
- [33] S. Li, Analyses and new designs of digital chaotic ciphers, Ph.D. thesis, School of Electronics and Information Engineering, Xi’an Jiaotong University, Xi’an, China, available online at <http://www.hooklee.com/pub.html> (June 2003).
- [34] A. Uhl, A. Pommer, *Image and Video Encryption: From Digital Rights Management to Secured Personal Communication*, Springer Science + Business Media Inc., Boston, 2005.
- [35] B. Furht, D. Socek, A. M. Eskicioglu, Fundamentals of multimedia encryption techniques, in: B. Furht, D. Kirovski (Eds.), *Multimedia Security Handbook*, CRC Press LLC, Boca Raton, Florida, 2004, Ch. 3, pp. 93–132.

- [36] S. Li, G. Chen, X. Zheng, Chaos-based encryption for digital images and videos, in: B. Furht, D. Kirovski (Eds.), *Multimedia Security Handbook*, CRC Press, LLC, 2004, Ch. 4, pp. 133–167, preprint available online at <http://www.hooklee.com/pub.html>.
- [37] R. L. Devaney, *An Introduction to Chaotic Dynamical Systems*, Addison-Wesley, Redwood City, California, USA, 1989.
- [38] T. Kohda, K. Aihara, Chaos in discrete systems and diagnosis of experimental chaos, *Trans. IEICE E73* (6) (1990) 772–783.
- [39] Wikipedia, Geometric distribution, online document available at http://en.wikipedia.org/wiki/Geometric_Distribution (2007).
- [40] B. Schneier, *Applied Cryptography – Protocols, algorithms, and source code in C*, 2nd Edition, John Wiley & Sons, Inc., New York, 1996.
- [41] C. Li, S. Li, D. Zhang, G. Chen, Cryptanalysis of a chaotic neural network based multimedia encryption scheme, in: *Advances in Multimedia Information Processing - PCM 2004 Proceedings, Part III*, Vol. 3333 of *Lecture Notes in Computer Science*, Springer-Verlag, 2004, pp. 418–425.